ЖУРНАЛ СТРУКТУРНОЙ ХИМИИ

2014. Том 55, № 3 *Май – июнь* *С. 553 – 556*

UDC 548.73:546.72:546.21

A NOVEL PROCESS FOR MAKING ALKALINE IRON OXIDE NANOPARTICLES BY A SOLVO THERMAL APPROACH

D. Mishra, R. Arora, S. Lahiri, S.S. Amritphale, N. Chandra

Council of Scientific and Industrial Research, Advanced Materials and Processes Research Institute, Bhopal, India
E-mail: ssamritphalerrl@yahoo.co.in

Received December, 26, 2012

In the present work alkaline iron oxide nanoparticles are synthesized by a novel solvo thermal approach and characterized exhaustively by various complementary techniques. Field emission scanning electron microscopy (FESEM) studies reveal that the size of nanoparticles is in the range of 31.5 nm to 96.9 nm. Energy-dispersive X-ray spectroscopy spectral analysis reveals the presence of oxygen, carbon, iron, and sodium. The X-ray diffraction studies confirm the formation of tetragonal $NaFeO_2$ as the major phase along with orthorhombic $NaFeO_2 \cdot H_2O$ and rhombohedral $FeCO_3$ (siderite) as the minor phases. Fourier transform infrared spectroscopy exhibits peaks due to the stretching and bending vibrations of O—H, C=O, CH_3—N, CH_3, C—H, C—N, and Fe—O groups. Differential scanning calorimetry (DSC) results display an endothermic peak at 100.85 °C and a very small endothermic peak at 791.56 °C with 819.73 mJ and 349.28 mJ energies respectively. These DSC peaks can be correlated with thermal gravimetric analysis (TGA) peaks representing 31.04 % weight loss and 7.70 % weight loss respectively in the sample at around 160 °C and 980 °C respectively.

K e y w o r d s: alkaline iron oxide, nanoparticles, solvo thermal.

INTRODUCTION

In recent years the synthesis of nanoparticles is of great scientific interest because of their unique properties and a wide application spectrum ranging from nanodevices[1], medical science [2], water purification [3], nanocomposites [4], chemical sensors [5] to magnetic materials [6]. Some of the common synthesis techniques for nanomaterials [7] includes the sol-gel method, the sonochemical method, the hydrothermal method, microbial synthesis, microwave assisted synthesis, microemulsion synthesis etc. Nano iron oxides are one of the important metal oxides because of their wide applications in pigments, anticorrosive agents, catalysts and also in *in-vivo* systems. Among various nano iron oxides, ferrites have attracted increasing attention due to their superior magnetization properties and high resistivity [8]. They possess a wide application spectrum in satellite communication, high capacity batteries, and low magnetization ferrofluids [9].

As reported by B.S. Randhawa *et al.* [9], the conventional ceramic method of the formation of ferrites suffers from disadvantages of a low surface area, non-homogeneity, and poor sinterability. In view of this, the present work has been undertaken, which involves the synthesis of alkaline iron oxide nanoparticles by a novel solvo thermal method using anhydrous ferric chloride, sodium hydroxide solution, ethylene glycol, and cetyl trimethyl ammonium bromide as a surfactant. This method overcomes the drawbacks of the conventional ceramic method.

Materials. Anhydrous ferric chloride, sodium hydroxide, and cetyl trimethyl ammonium bromide (CTAB) were procured from Rankem and ethylene glycol was procured from Merck and used as such

© Mishra D., Arora R., Lahiri S., Amritphale S.S., Chandra N., 2014

without further purification. All reagents were of analytical grade and double distilled water was used for the preparation of an aqueous solution as well as for the washing purpose.

Synthesis of alkaline iron oxide nanoparticles. Alkaline iron oxide nanoparticles have been synthesized by a solvo thermal method. Ferric chloride was used as an iron ion source. Its aqueous solution (25 g in 25 ml) was refluxed with sodium hydroxide (3M aqueous solution in 250 ml) and ethylene glycol (62.5 ml) in the presence of CTAB (1.25 g) as a surfactant at a temperature around 198 °C to 200 °C for 58 hours. Excess of ethylene glycol was recovered back by distillation and the system was allowed to cool at the end of the reaction at ambient temperature. The resultant product was collected at the bottom of flask in the form of a reddish brown colored gel. The gel obtained was washed repeatedly and extensively with water and finally with acetone for three times and dried at room temperature.

Characterization. An X-ray diffraction pattern was obtained on a D8 ADVANCE X-ray diffractometer using CuK_α radiation to determine different phases. The X-ray diffraction intensity was recorded as a function of Bragg′s 2θ in the angular range 5—70°. IR spectra were taken using a Bruker alpha Fourier Transform Infra Red Spectrometer to determine the functional group present in the samples in the range 500—4000 cm^{-1}. Field emission scanning electron microscope (FESEM), model NOVA NANOSEM-430 of COMFEI and energy dispersive X-ray spectroscopy (EDX), Model X-MAX of Oxford were used for the determination of the morphology and microstructure. The sample was sonicated for a period of 15 min in acetone before mounting for FESEM and EDX. Thermal gravimetric analysis (TGA) and differential scanning calorimetry (DSC) analysis were performed on Toledo TGA/ DSC-1 of Mettler Company by heating the sample at a heating rate of 10 °C/ min from 30 °C to 1200 °C under the nitrogen atmosphere to determine the thermal properties of nanoparticles.

RESULTS AND DISCUSSION

X-Ray diffraction studies. The X-ray diffraction (XRD) pattern of synthesized alkaline iron oxide nanoparticles is given in Fig. 1. The experimentally obtained d values were compared with the standard d values in JCPDS data [10].

The XRD peaks observed at a d value of 2.82, 2.64, 1.99 and 1.62 confirmed the formation of $NaFeO_2$ as the major phase (tetragonal, 2.84, 2.64,1.95 and 1.67, JCPDS file number 30-1196) along with $NaFeO_2 \cdot H_2O$ (orthorhombic, 2.83, 2.62, and 2.00, JCPDS fie number 21-1127) and $FeCO_3$ (siderite, rhombohedral, 2.79 and 1.96, JCPDS file number 29-696) as the minor phases. The presence of peaks for NaCl (halite, cubic, 2.82, 1.99 and 1.62, JCPDS file number 5-628) as impurity are also observed from XRD. The XRD peaks due to $FeCO_3$ are observed due to the carbonation of alkaline iron species which generally are nanomaterials absorbed from the environment due to their high surface area [11].

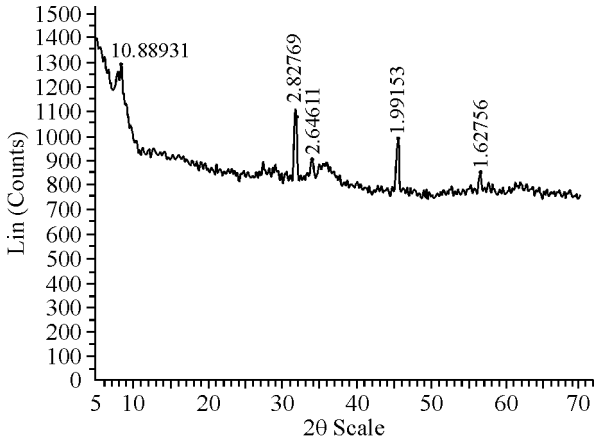

Fig. 1. XRD pattern obtained for synthesized alkaline iron oxide nanoparticles

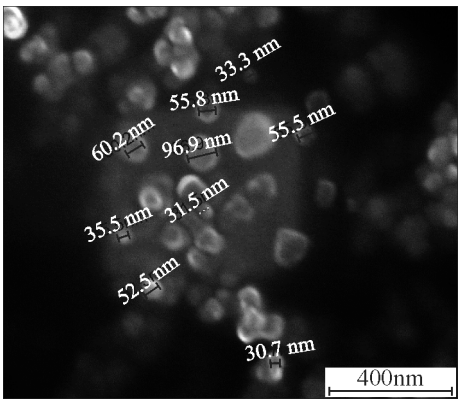

Fig. 2. FESEM image of synthesized alkaline iron oxide nanoparticles

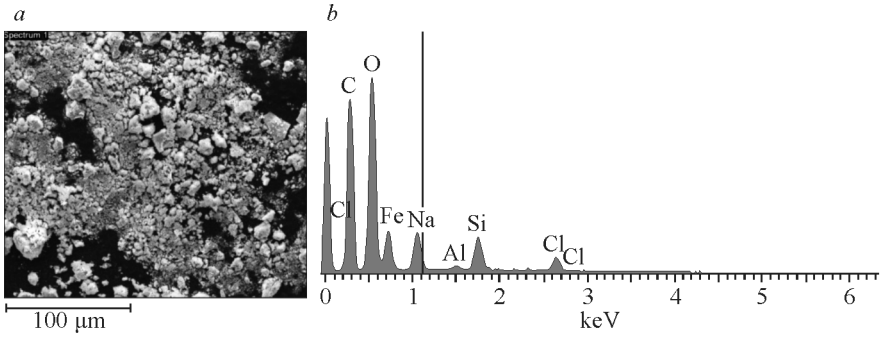

Element	Weight, %	Atomic, %
C *K*	35.11	52.50
O *K*	29.33	32.93
Na *K*	3.52	2.75
Al *K*	0.26	0.17
Si *K*	3.16	2.02
Cl *K*	2.33	1.18
Fe *L*	26.29	8.45
Totals	100.00	

Fig. 3. EDX spectra of synthesized alkaline iron oxide nanoparticles: selected area (*a*); EDX outcomes (*b*); elemental compositions (*c*) (weight % and atomic %)

FESEM studies. The morphology of the synthesized material was studied using FESEM as shown in Fig. 2 and EDX spectra are shown in Fig. 3. Several particles were investigated to determine the particle size. It has been observed that the particles are well dispersed and almost spherical in shape with a particle size ranging from about 31.5 nm to 96.9 nm. The EDX spectral analysis reveals the predominance of carbon, oxygen, iron, and sodium with their weight composition of 35.11 %, 29.33 %, 26.29 %, and 3.52 % respectively in the synthesized nanoparticles. The appearance of a peak of carbon in the EDX spectra is due to the presence of organic linkages due to ethylene glycol and CTAB.

FTIR studies. FTIR spectra of the synthesized alkaline oxide nanoparticles are presented in Fig. 4. It displays bands due to the stretching and bending vibrations of O—H (3844—3615 cm^{-1} and 2360 cm^{-1}), C=O (1741 cm^{-1} and 1691 cm^{-1}), CH_3—N (1647cm^{-1}), CH_3 (1461 cm^{-1}), C—H (1515 cm^{-1}), C—N (1031 cm^{-1}), and Fe—O (877 cm^{-1}, 520 cm^{-1}, 447 cm^{-1}, and 402 cm^{-1}) groups, which are in agreement with the reported values [12, 13].

Thermal analysis. TGA and DSC of alkaline iron oxide nanoparticles are shown in Fig. 5.

DSC results display endothermic peaks in the temperature range of 90.21 °C to 100.85 °C and a very small endothermic peak in the temperature range of 784.78 °C to 791.56 °C and is associated with 819.73 mJ (35.66 J/gm) and 349.28 mJ (15.19 J/gm) of energies respectively. These DSC peaks can be correlated with TGA peaks representing 31.04 % and 7.70 % weight loss at 160 °C and 980 °C respectively in the sample.

The first TGA peak can be ascribed to the loss of moisture and volatile matter and the second peak can be ascribed to the decarbonation of $FeCO_3$ [14, 15] formed due to the absorption of carbon dioxide and water from the environment, as also indicated by the peak of $FeCO_3$ in the XRD pattern of the synthesized nanoparticles. The weight loss due to the decarbonation of $FeCO_3$ is also confirmed by the mass balance equation below indicating around 37.60 % weight loss in the sample which matches with TGA values representing total 37.93 % weight loss in the sample:

$FeCO_3$ (molecular weight = 116) → FeO (molecular weight = (72) + CO_2 (molecular weight = 44).

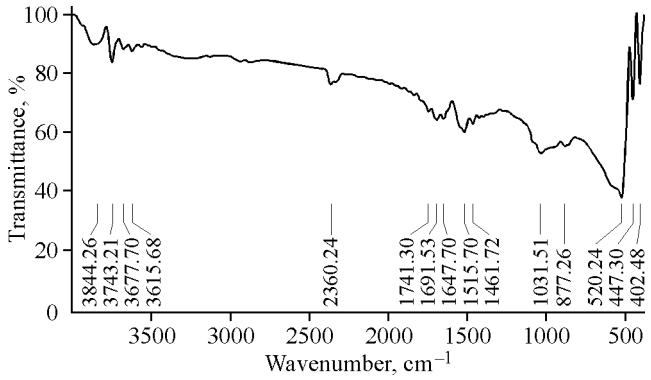

Fig. 4. FTIR spectra of synthesized alkaline iron oxide nanoparticles

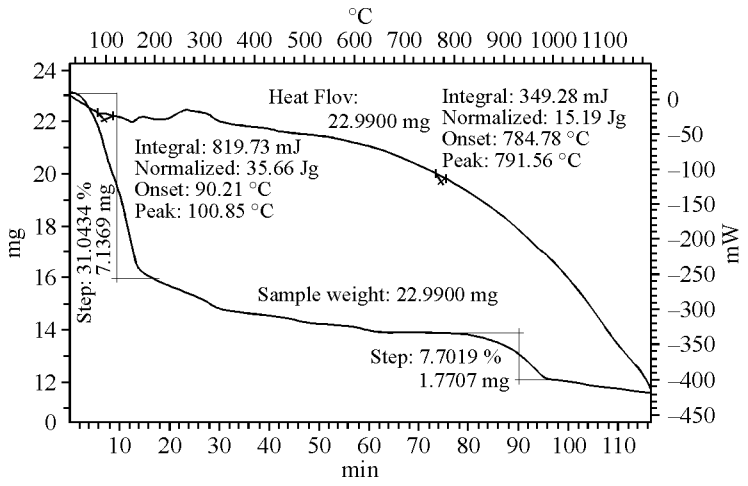

Fig. 5. TGA and DSC curves of synthesized alkaline iron oxide nanoparticles

CONCLUSIONS

Alkaline iron oxide nanoparticles were synthesized successfully by a novel solvo thermal technique obviating the need of sintering as used in the conventional ceramic route for the synthesis of ferrites. The characterisation of synthesized nanoparticles was made exhaustively using various sophisticated complementary techniques. The XRD studies confirmed the formation of $NaFeO_2$ as the major phase along with $NaFeO_2 \cdot H_2O$ and $FeCO_3$ as the minor phases. The FESEM studies reveal that the nanoparticles are almost spherical in shape with a particle size in the range of about 31.5 nm to 96.9 nm. The EDX spectral analysis revealed the predominance of oxygen, carbon, iron, and sodium apart from iron-containing alkaline species. FTIR spectra displayed the bands due to the stretching and bending vibrations of O—H, C=O, CH_3—N, CH_3, C—H, C≡N, and Fe—O groups. The TGA analysis indicated around 37.93 % loss in weight due to the dehydroxylation and decarbonation of $FeCO_3$.

Acknowledgements. The authors are grateful to Director CSIR-AMPRI Bhopal for providing necessary institutional facilities and encouragement. Thanks are also due to Dr. O.P. Modi, Mr. Anup Khare, and Mr. Mohd. Shafique, CSIR-AMPRI for the analysis of samples on FESEM and EDX and providing data on the thermal analysis of thesamples, to Dr. S. Das, CSIR-AMPRI for providing facilities for X-ray diffraction analysis, and to Dr Neelesh Jain, SIRT, Bhopal for providing facilities for IR spectra.

REFERENCES

1. *Shklover V., Hofmann H.* – P. 181 – 192. Handbook of Semiconductor Nanostructures, Nanodevices Edited, 2006. – **2**. – P. 181 – 213.
2. *Zhang L., Gu F.X., Chan J.M., Wang A.Z., Langer R.S., Farokhzad O.C.* // Clin. Pharmacol. Ther. – 2008. – **83**, N 5. – P. 761 – 69.
3. *Pradeep T., Anshup.* // Thin Solid Films. – 2009. – **517**. – P. 6441 – 6478.
4. *Kong P.C., Kawczak Alex W.* Sep 01 2008. 8th World Congress Nanocomposites, DE-AC07-99ID-137.
5. *Yoon H., Chang M., Jang J.* // Advanced Functional Materials. – 2007. – **17**, N 3. – P. 431 – 436.
6. *Vatta L.L, Sanderson R.D., Koch K.R.* // Pure Appl. Chem. – 2006. – **78**, N 9. – P. 1793 – 1801.
7. *Tavakoli A., Sohrabi M., Kargari A.* // Chem. Pap. – 2007. – **61**, N 3. – P. 151 – 170.
8. *Randhawa B.S., Gandotra K.* // Ceramics International. – 2009. – **35**, N 1. – P. 157 – 161.
9. *Randhawa B.S., Kamaljeet S.* // J. Radioanalytical, Nuclear Chemistry. – 1998. – **238**, N 1-2. – P. 141 – 144.
10. *Powder* Diffraction File, Alphabetical Index Inorganic Phases JCPDS International Centre For Diffraction Data, Pennsylvania, 1984.
11. *Rahman M.M., Khan S.B., Jamal A., Faisal M., Aisiri A.M.* Iron Oxide Nanoparticles, Nanomaterials / Ed. M.M. Rahman, 2011. http: // www.intechopen.com/articles/show/title/iron-oxide-nanoparticles
12. *Coates J.* Interpretation of Infrared Spectra, A Practical Approach in Encyclopedia of Analytical Chemistry / Ed. A. Meyers. John Wiley & Sons Ltd, Chichester. – 2000. – P. 10815 – 10837.
13. *Farmer V.C.* The Infrared Spectra of Minerals Monograph 4. – L.: Mineralogical Society, 1974.
14. *Bell M.S., Lin I.-C., Mckay D.S.* Analysis of Siderite Thermal Decomposition By Differential Scanning Calorimetry., Catastrophic Events Conference 3117.Pdf
15. *Wang J., Sakakura T., Ishizawa N., Eba H.* IOP Conf. Series: Materials Science, Engineering. 2011-18-022011 (http://iopscience.iop.org/1757-899X/18/2/022011).